

## $\alpha$ -Benzoin Oxime in Higher Oxidation State 3d Metal Cluster Chemistry: Structural and Magnetic Study of a New $\text{Mn}^{\text{III}}_9$ Complex

Evangelia S. Koumoussi,<sup>†</sup> Manolis J. Manos,<sup>‡</sup> Christos Lampropoulos,<sup>§</sup> Anastasios J. Tasiopoulos,<sup>‡</sup> Wolfgang Wernsdorfer,<sup>⊥</sup> George Christou,<sup>\*,§</sup> and Theodoros C. Stamatatos<sup>\*,†</sup>

<sup>†</sup>Department of Chemistry, University of Patras, Patras 26504, Greece, <sup>‡</sup>Department of Chemistry, University of Cyprus, 1678 Nicosia, Cyprus, <sup>⊥</sup>Institut Néel, CNRS, BP166, 38042 Grenoble Cedex 9, France, and <sup>§</sup>Department of Chemistry, University of Florida, Gainesville, Florida 32611-7200

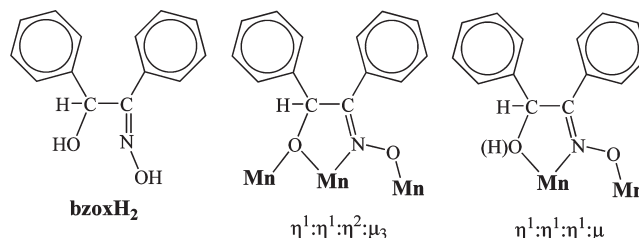
Received January 29, 2010

The initial employment of  $\alpha$ -benzoin oxime ( $\text{bzoxH}_2$ ) in higher oxidation state 3d metal cluster chemistry has provided access to a new enneanuclear  $\text{Mn}^{\text{III}}$  complex with an unprecedented metal-core topology consisting of two triangular  $[\text{Mn}_3(\mu_3\text{-O}^2-)(\mu\text{-ON})_3]^{4+}$  fragments connected by a linear  $[\text{Mn}_3(\mu\text{-ON})_6]^{3+}$  unit. The  $\text{Mn}^{\text{III}}_9$  cluster is antiferromagnetically coupled and has an  $S = 3$  spin ground state.

There are multiple reasons for the current interest by groups around the world in the synthesis and study of high-nuclearity 3d molecular metal clusters at moderate oxidation states. Among these is the search for various nuclearity oxide-bridged metal clusters to model  $\text{M}_x$  sites in biomolecules, including understanding the growth of the core of the ferritin protein and synthesis of the Mn site of water oxidation within the photosynthetic apparatus of green plants and cyanobacteria.<sup>1</sup> In addition, high-nuclearity 3d metal clusters often display interesting and occasionally novel magnetic properties, including high-spin ( $S$ ) ground-state values, currently up to  $83/2$ ,<sup>2</sup> and single-molecule magnet (SMM) behavior.<sup>3</sup> The latter results in molecules with a ground state of a high magnetic moment, which also exhibits an important axial anisotropy.

Crucial to such efforts and others is the continuing development of new synthetic routes to high-nuclearity species with unprecedented structural topologies. However, there is no obvious and guaranteed procedure to such species.<sup>4</sup> Much work over the last 10 years has been invested in exploring different strategies, and there are now several empirically established approaches to a variety of molecular species. Among these is the use of hydrolysis and alcoholysis reactions in the presence of carboxylate groups, with or without

**Chart 1.** Structure of  $\alpha$ -Benzoin Oxime (Left) and the Binding Modes of Its Monoanion ( $\text{bzoxH}^-$ ) and Dianion ( $\text{bzox}^{2-}$ ) in Complex **1** (Middle and Right)



chelating ligands.<sup>5</sup> Another attractive approach is to use chelates containing alkoxide or oximate functionalities because these are good bridging groups that can foster the formation of polynuclear products with various structural motifs and interesting magnetic properties, including high-spin molecules and SMMs.<sup>6</sup>

As an extension to this approach, we have recently turned our attention to a new mixed alkoxide–oximate ligand, namely,  $\alpha$ -benzoin oxime ( $\text{bzoxH}_2$ ; Chart 1), in 3d metal cluster chemistry as a potentially new route to high-nuclearity molecular species with unprecedented structural topologies and interesting physical properties. Efforts to date by us<sup>7a</sup> and others<sup>7b</sup> with  $\text{bzoxH}_2$  have been solely in divalent 3d metal chemistry, yielding products such as  $\text{Cu}^{\text{II}}_{10}$ <sup>7a</sup> and  $\text{Ni}^{\text{II}}_8$  and  $\text{Ni}^{\text{II}}_6$ ,<sup>7b</sup> all with a similar loop or single-strand wheel topology. We herein report the initial employment of  $\text{bzoxH}_2$  in trivalent 3d metal cluster chemistry, which has provided access to a new enneanuclear  $\text{Mn}^{\text{III}}$  complex with an interesting topology containing both the mono- and dianionic forms of the ligand,  $\text{bzoxH}^-$  and  $\text{bzox}^{2-}$ , respectively. We

(5) Christou, G. *Polyhedron* **2005**, *24*, 2065 and references cited therein.

(6) (a) Brechin, E. K. *Chem. Commun.* **2005**, 5141. (b) Milios, C. J.; Stamatatos, Th. C.; Perlepes, S. P. *Polyhedron* **2006**, *25*, 134. (c) Tasiopoulos, A. J.; Perlepes, S. P. *Dalton Trans.* **2008**, 5537. (d) Milios, C. J.; Piligkos, S.; Brechin, E. K. *Dalton Trans.* **2008**, 1809.

(7) (a) Vlahopoulou, G. C.; Stamatatos, Th. C.; Psycharis, V.; Perlepes, S. P.; Christou, G. *Dalton Trans.* **2009**, 3646. (b) Karotsis, G.; Stoumpos, C. C.; Collins, A.; White, F.; Parsons, S.; Slawin, A. M. Z.; Papaefstathiou, G. S.; Brechin, E. K. *Dalton Trans.* **2009**, 3388.

\*To whom correspondence should be addressed. E-mail: thstama@chemistry.upatras.gr.

(1) Barber, J.; Murray, J. W. *Coord. Chem. Rev.* **2008**, *252*, 416.

(2) Ako, A. M.; Hewitt, I. J.; Mereacre, V.; Clérac, R.; Wernsdorfer, W.; Anson, C. E.; Powell, A. K. *Angew. Chem., Int. Ed.* **2006**, *45*, 4926.

(3) Gatteschi, D.; Sessoli, R. *Angew. Chem., Int. Ed.* **2003**, *42*, 268.

(4) Winpenny, R. E. P. *J. Chem. Soc., Dalton Trans.* **2002**, 1.

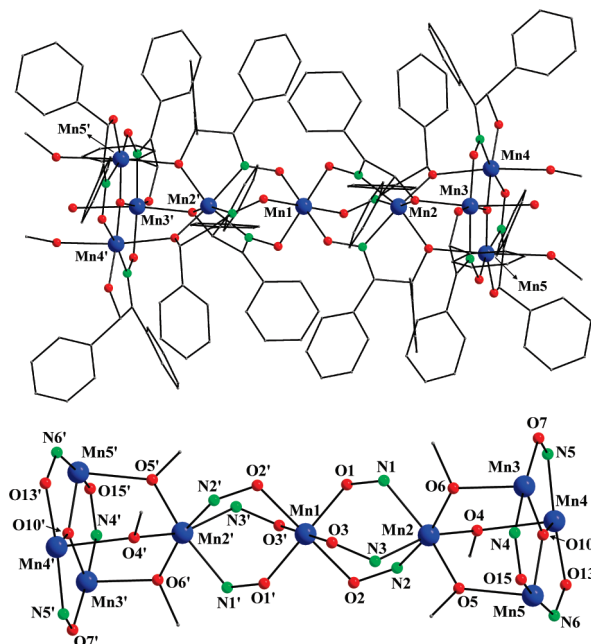


**Figure 1.** Labeled PovRay representation of complex **1**, with H atoms omitted for clarity (top) and its  $[\text{Mn}_9(\mu_3\text{-O})_2(\mu\text{-OR})_6(\mu\text{-ON})_{12}]^{3+}$  core (bottom). Color scheme:  $\text{Mn}^{\text{III}}$ , blue; O, red; N, green; C, gray. Primes are used for symmetry-related atoms.

believe this compound is the prototype of a rich new area of polynuclear metal clusters at such high oxidation states as  $\text{Mn}^{\text{III}}$ , derived from the amalgamation of oximate and alkoxide groups within the same ligand.<sup>8</sup>

The reaction of  $\text{Mn}(\text{NO}_3)_2 \cdot \text{H}_2\text{O}$ ,  $\text{bzoxH}_2$ , and  $\text{NEt}_3$  in a 2:3:3 molar ratio in MeOH gave a dark-brown solution that upon slow evaporation at room temperature for several days gave dark-red crystals of  $[\text{Mn}_9\text{O}_2(\text{bzox})_{11}(\text{bzoxH})(\text{MeOH})_4(\text{H}_2\text{O})_2] \cdot 14\text{MeOH}$  (**1**·14MeOH) in 55% yield.<sup>9</sup> The molecular structure of **1** (Figure 1, top) comprises nine  $\text{Mn}^{\text{III}}$  ions linked through two  $\mu_3\text{-O}^{2-}$  ions (O10 and O10') and the oximate  $\text{N}-\text{O}^-$  and alkoxide  $\text{RO}^-$  arms of 11  $\text{bzox}^{2-}$  and 1  $\text{bzoxH}^-$  groups. The core of **1** consists of a central, linear  $[\text{Mn}_3^{\text{III}}(\mu\text{-ON})_6]^{3+}$  unit (Mn1, Mn2, and Mn2') attached to two  $[\text{Mn}_3^{\text{III}}(\mu_3\text{-O})(\mu\text{-ON})_3]^{4+}$  triangular units (Mn3, Mn4, Mn5, Mn3', Mn4', and Mn5') at each end. The ligation between the linear  $\text{Mn}_3$  unit and the two  $\text{Mn}_3$  triangles is provided by six monatomic  $\text{RO}^-$  bridges (O4, O5, O6, O4', O5', and O6') from six different  $\text{bzox}^{2-}$  groups to give an overall  $[\text{Mn}_9(\mu_3\text{-O})_2(\mu\text{-OR})_6(\mu\text{-ON})_{12}]^{5+}$  core (Figure 1, bottom). The  $\text{bzox}^{2-}$  and  $\text{bzoxH}^-$  groups bind in  $\eta^1:\eta^1:\eta^2:\mu_3$  and  $\eta^1:\eta^1:\eta^1:\mu$  modes (Chart 1). Peripheral ligation about the core is provided by six terminal alkoxo O atoms that belong to the “chelating” parts of the organic ligands and four and two terminal MeOH and  $\text{H}_2\text{O}$  molecules at  $\text{Mn}(4,4',5,5')$  and  $\text{Mn}(3,3')$ , respectively.

All Mn atoms are six-coordinate with distorted octahedral geometry. The metal oxidation states and the protonation

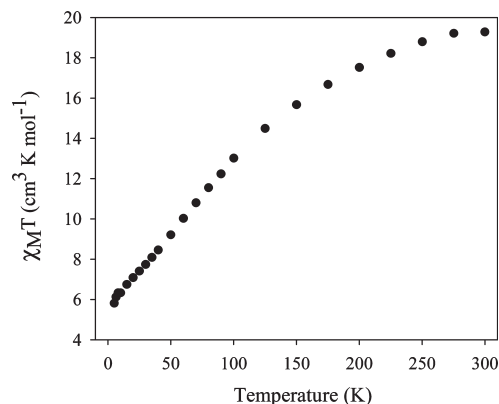


**Figure 2.** Plot of  $\chi_{\text{M}}T$  vs  $T$  for complex **1** in a 1 kG dc field.

levels of  $\text{O}^{2-}/\text{RO}^-$  ions were deduced from the metric parameters and charge-balance considerations and were confirmed by bond valence sum (BVS) calculations<sup>10</sup> and the presence of Jahn–Teller (JT) axial elongations at  $\text{Mn}(1,3,4,5,1',3',4',5')$ .<sup>11</sup> In the case of  $\text{Mn}(2,2')$ , the absence of a clear JT axis is assigned to its static disorder among the three virtually symmetry-equivalent  $\text{O}(4,5,6)-\text{Mn}(2)-\text{N}(2,1,3)$  axes.<sup>12</sup> As a result of the Mn and O BVS calculations, the formula of **1** initially appeared to be  $[\text{Mn}^{\text{III}}_9\text{O}_2(\text{bzox})_{12}(\text{MeOH})_4(\text{H}_2\text{O})_2]^+$ , with its monocationic nature disagreeing with the absence of a counteranion. To maintain the neutral charge of the cluster, it is very likely that the crystallographic  $C_i$  symmetry of the molecule is masking the presence of a proton statically disordered between a  $\text{bzox}^{2-}/\text{bzoxH}^-$  pair or even among several such groups. As has been previously observed in other 3d metal/oximate clusters,<sup>13</sup> a static disorder of an  $\text{H}^+$  ion over two or more sites would average out its influence on the structural parameters and thus make it very difficult to detect.

Complex **1** is the first structurally characterized 3d metal complex in the oxidation state III to contain any form (neutral or mono- or dianionic) of the  $\alpha$ -benzoin oxime ligand and possesses an unprecedented structural motif among the various reported  $\text{Mn}_9$  clusters at any oxidation level. Complex **1** also joins only a handful of previous  $\text{Mn}^{\text{III}}$  clusters with a nuclearity of 9,<sup>14</sup> none of which have structures similar to that of **1**.

Solid-state direct-current (dc) magnetic susceptibility ( $\chi_{\text{M}}$ ) data were collected on **1** in a 1 kG (0.1 T) field in the 5.0–300 K range. The obtained data are plotted as  $\chi_{\text{M}}T$  versus  $T$  in Figure 2:  $\chi_{\text{M}}T$  steadily decreases with decreasing temperature from  $19.30 \text{ cm}^3 \text{ K mol}^{-1}$  at 300 K to  $5.80 \text{ cm}^3 \text{ K mol}^{-1}$  at 5 K, suggesting predominantly antiferromagnetic interactions between the metal centers.  $\chi_{\text{M}}T$  at 5 K suggests that **1** possesses a small, but nonzero, ground-state spin  $S$ .

(10) Liu, W.; Thorp, H. H. *Inorg. Chem.* **1993**, *32*, 4102. BVS for the  $\text{Mn}^{3+}$  and  $\text{O}^{2-}$  were 2.93–3.30 and 1.99, respectively.

(11) See the Supporting Information.

(12) Fackler, J. P.; Avdeef, A. *Inorg. Chem.* **1984**, *13*, 1864.

(13) (a) Stoumpos, C. C.; Stamatatos, Th. C.; Sartzi, H.; Roubeau, O.; Tasiopoulos, A. J.; Nastopoulos, V.; Teat, S. J.; Christou, G.; Perlepes, S. P. *Dalton Trans.* **2009**, 1004. (b) Weyhermüller, Th.; Wagner, R.; Khanra, S.; Chaudhuri, P. *Dalton Trans.* **2005**, 2539.

(14) (a) Brechin, E. K.; Christou, G.; Soler, M.; Helliwell, M.; Teat, S. J. *Dalton Trans.* **2003**, 513. (b) Chakov, N. E.; Zakharov, L. N.; Rheingold, A. L.; Abboud, K. A.; Christou, G. *Inorg. Chem.* **2005**, *44*, 4555. (c) Lampropoulos, C.; Stamatatos, Th. C.; Abboud, K. A.; Christou, G. *Polyhedron* **2009**, *28*, 1958 and references cited therein.

(8) Price, D. J.; Batten, S. R.; Berry, K. J.; Moubaraki, B.; Murray, K. S. *Polyhedron* **2003**, *22*, 165.

(9) Anal. Calcd (found) for dried **1** (solvent-free): C, 60.86 (60.95); H, 4.54 (4.63); N, 4.95 (4.86). Crystal structure data for **1**·14MeOH:  $\text{C}_{186}\text{H}_{174}\text{Mn}_9\text{N}_{12}\text{O}_{46}$ ,  $M_w = 3807.83$ , triclinic, space group  $P1$  with  $a = 14.6788(4) \text{ \AA}$ ,  $b = 16.0304(5) \text{ \AA}$ ,  $c = 20.8869(6) \text{ \AA}$ ,  $\alpha = 99.207(2)^\circ$ ,  $\beta = 100.439(2)^\circ$ ,  $\gamma = 106.774(3)^\circ$ ,  $V = 4508.7(2) \text{ \AA}^3$ ,  $T = 100(2) \text{ K}$ ,  $Z = 1$ ,  $R1 [I > 2\sigma(I)] = 0.0702$ ,  $wR2 = 0.1891$  ( $F^2$ , all data).

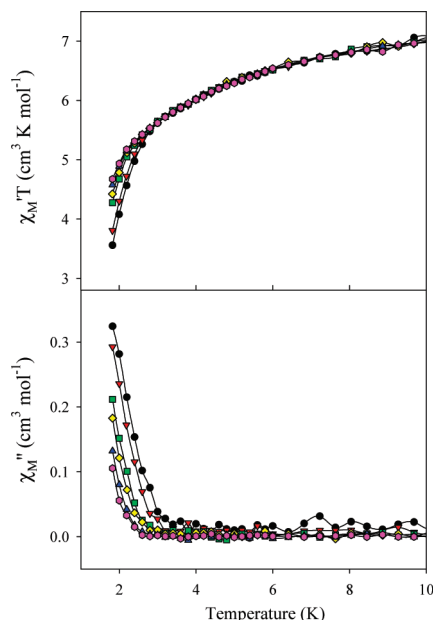


**Figure 3.** In-phase ( $\chi_M'$ ; as  $\chi_M' T$ , top) and out-of-phase ( $\chi_M''$ , bottom) vs  $T$  ac susceptibility signals for **1** in a 3.5 G field oscillating at frequencies in the 1500–25 Hz range.

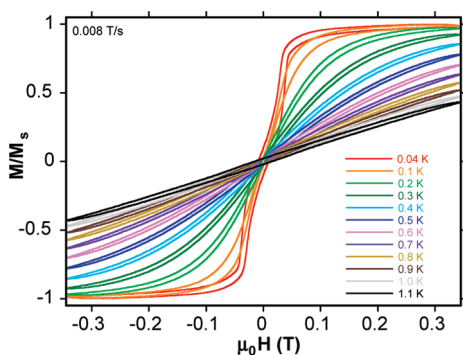


**Figure 4.** Magnetization ( $M$ ) vs dc field hysteresis loops for a single crystal of **1**·14MeOH at the indicated temperatures and a fixed field sweep rate of 0.008 T s<sup>−1</sup>. The magnetization is normalized to its saturation value,  $M_S$ .

A theoretical treatment of the susceptibility data using the Kambe approach was not feasible because of the topological complexity and low symmetry of **1**. Instead, our efforts focused on the determination of the  $S$  value of **1** by variable-temperature and -field magnetization ( $M$ ) measurements in the 1.8–10.0 K and 0.1–7 T ranges, respectively. Attempted fits of the data, assuming that only the ground state is populated, were poor,<sup>11</sup> suggesting complications from low-lying excited states even at these relatively low temperatures.

As we have described before on multiple occasions, alternating-current (ac) susceptibility studies are a powerful complement to dc studies for determining the ground state

of a system. We thus carried out ac studies on complex **1** to obtain its ground state  $S$  and also to study its magnetization dynamics. The in-phase ( $\chi_M'$ ) ac signal, shown as  $\chi_M' T$  in Figure 3 (top), is very temperature-dependent in the 4–10 K region, confirming the conclusion from the dc studies of many very low-lying excited states, with  $S$  larger than the ground state. Extrapolating the plot above 4 K down to 0 K gives a value of  $\sim 5.8$  cm<sup>3</sup> K mol<sup>−1</sup>, suggesting an  $S = 3$  ground state with  $g$  slightly less than 2.0, as expected for Mn<sup>III</sup> clusters. Below 4 K, complex **1** displays a frequency-dependent decrease in  $\chi_M' T$  and a concomitant appearance of out-of-phase  $\chi_M''$  signals (Figure 3, bottom).

The  $\chi_M''$  signals in Figure 3 (bottom) suggest, but do not prove, that complex **1** is a SMM. To confirm this, magnetization versus dc field sweeps were performed, on a single crystal of **1**·14MeOH at temperatures below 1.8 K using a micro-SQUID apparatus,<sup>15</sup> to look for magnetization hysteresis, the diagnostic property of a magnet. The temperature dependence at a fixed sweep rate of 0.008 T s<sup>−1</sup> is shown in Figure 4. Hysteresis loops become evident in the scans at 1.1 K, but they only have a small coercivity. The latter is essentially constant with decreasing temperature down to 0.04 K. Figure S4 in the Supporting Information shows the sweep-rate dependence of the loops at a constant temperature of 0.04 K. A small decrease in coercivity is observed with a decreasing sweep rate, but again the change is only slight. This behavior is *not* what was expected for a SMM, for which one would expect a greater dependence of the coercivity on the temperature and on the sweep rate. A closer inspection of the loops in Figure 4, and particularly the shift of the first step at negative fields, is indicative of magnetization relaxation phenomena that arise from antiferromagnetic intermolecular interactions between neighboring Mn<sub>9</sub> clusters; this is indeed supported by the presence of Mn<sub>9</sub>–(MeOH)<sub>lattice</sub>–Mn<sub>9</sub> interactions in the crystal structure of **1**·14MeOH.<sup>11</sup>

In conclusion, we report the initial use of  $\alpha$ -benzoin oxime (bzoXH<sub>2</sub>) in higher oxidation state 3d metal chemistry, which has afforded an unusual enneanuclear Mn<sup>III</sup> cluster with an unprecedented topology based on linear and triangular Mn<sub>3</sub> units. This prototype product suggests that future reactions of this ligand with other M<sup>3+</sup> ions promises to deliver many new and exciting molecular species with interesting structural and magnetic properties.

**Acknowledgment.** This work was supported by the Cyprus Research Promotion Foundation, the National Science Foundation (Grant CHE-0910472), and ERC Ad. Grant MolNanoSpin (226558).

**Supporting Information Available:** Crystallographic data for **1**·14MeOH in CIF format and various structural and magnetic figures. This material is available free of charge via the Internet at <http://pubs.acs.org>.

(15) Wernsdorfer, W. *Supercond. Sci. Technol.* **2009**, *22*, 064013.